

A new method for measuring the liquid permeability of coated and uncoated papers and boards

Cathy J. Ridgway, Joachim Schoelkopf and Patrick A.C. Gane, Omya AG, CH-4665 Oftringen, Switzerland

Keywords: paper permeability, measurement of permeability, porosity, pore structure, flow through porous media, permeability hysteresis.

SUMMARY

A new permeation apparatus is described to measure the liquid permeability of coated and uncoated paper samples. The technique can also be applied to other consolidated porous and laminate materials and removes the artefacts of random pinholes whilst relating directly to liquid permeation rather than the more commonly used air/gas permeation. Measurements from three example papers are shown, and the equivalent permeation radii and Darcy permeabilities are calculated. Liquid permeability is compared with both air permeability using the Bendtsen method and mercury porosimetry data for the same samples. Each method is shown to indicate different properties of the porous structures, i.e. porosity and equivalent intrusion diameter alone are not necessarily representative of the saturated permeability characteristics of a porous sample. Furthermore, the permeability of low permeable coated grades is underestimated using the commonly applied air method due to compression of the air causing non-linearity of the pressure gradient. It is necessary to consider network structures including connectivity and pore size and shape distributions in order to correlate porosimetry with liquid permeation properties of differing samples.

Address of the authors: Omya AG, CH-4665 Oftringen, Switzerland

INTRODUCTION AND BACKGROUND

In paper science and in industrial quality control, a permeability value is traditionally obtained by transplanar air permeation through a paper sheet. Specialised permeation methods are also applied, mainly in the medical, personal care and cigarette industries, such as that reported by Brown and Williamson Tobacco Corporation, Lorillard Tobacco Company and Philip Morris USA, using a Filtrona Paper Permeability Meter (PPM 100) to determine the air permeability (Borgerding et al. 2000). For the print media industry similar methods are widely used (Gurley-Hill S-P-S tester, (ISO 1994; 2001a) or the L&W Bendtsen tester, (Heinemann 1996; 2001b)) although there are some recognised major drawbacks. One is the compressibility of the air, another is turbulent flow induced by the low viscosity of the fluid as it passes through the strictures of the fibre mat and/or coating structure. Furthermore, as the air flow is measured through a relatively large area of the sheet, there is the danger that it passes preferentially through a local weak spot in the structure, for example through a pinhole or where there is a weakly bonded floc of fibres. This may also occur in the case of coated papers, especially if the paper has a region of low coat weight and the base paper coverage is incomplete. Liquid permeability, on the other hand, is mainly used to determine dewatering properties of the forming paper web and uncoated papers, as recently reviewed by Vomhoff *et al.* (Vomhoff et al. 2000). The majority of these methods measure only one sheet of paper and need a support for the paper sample in the form of a wire mesh, sintered metal plate or felt. Although these methods remove the problem of the compressibility of air the other drawbacks are still present. The method developed and introduced here, although more time consuming, overcomes many of the uncertainties and is also applicable to other porous planar substrates. Furthermore, it uses the flow of a liquid rather than a gas, and so is highly relevant to absorption and permeation of liquids in both the paper making and printing processes. The example liquid used here is an apolar mineral oil and, therefore, does not interact with the fibres nor with most latex coating binders (Rousu et al. 2001), which would otherwise affect the structural properties of the web and coating layer.

A large number of small sample sheets of each test sample are embedded in a resin block. By using such a stack of so many sheets, the dominating effect of pinholes or poor coating coverage can be avoided. Application of the Poiseuille equation, Eq. [1], provides a relationship between permeation rate, $d(V(t)/A)/dt$, defined as the flux or volume flow rate per

unit cross-sectional area, A , and the equivalent permeation radius for this unit cross-section, r_{perm} ;

$$\frac{d(V(t)/A)}{dt} = \frac{\pi r_{\text{perm}}^4 \delta P}{8\eta l} \quad [1]$$

where δP is the applied pressure difference across the sample, η is the viscosity of the liquid and l is the length of the sample, which, in this case of a compact of laminates, requires to be corrected for the occurrence of gaps between the sheets. In this equation, r_{perm} is the radius of an equivalent Poiseuille tube delivering the measured flux, $d(V(t)/A)/dt$, through a unit area of the sample. This permeation equation has been widely adopted and adapted to various situations, such as the recent application to the permeability of a growing filtercake of particles (Lohmander et al. 1999), which is similarly handled for the permeability of a fibre mat as the basis of paper making.

Alternatively, the continuous flow can be expressed in terms of the Darcy permeability constant, k , as,

$$\frac{dV(t)}{dt} = \frac{-kA\delta P}{\eta l} \quad [2]$$

In petroleum and soil science, work has been carried out to determine the spatial permeability, mostly on the macro scale, using k in the form of a 3-D permeability tensor, K_{ij} (Torsaeter, Abrahi 2000; van Brakel 1975). In the petroleum industry, the relative permeability of a fluid is of interest as a function of the saturation level of a second different fluid phase in the porous medium. In this work, the transplanar permeability of a thin substrate, such as paper, is investigated and an absolute z -direction permeability value determined, $k = K_{33}$.

Comparison is made between the permeability results and the findings obtained using mercury intrusion porosimetry. A clear discrepancy between the descriptors of a porous structure in the simplistic terms of porosity and equivalent intrusion pore diameter, and the observed equilibrium permeability occurring between structures of different forms, i.e. between uncoated and coated papers and between uncoated papers of different types, is used to highlight the necessity to consider the properties of networks and not to assume that porous media can be described by a simple bundle of parallel capillaries.

EXPERIMENTAL METHOD (NOVEL DEVELOPMENT)

Sample preparation

A stack of paper/board samples (approximately 125 sheets) is placed into a mould¹ under a slight overpressure, applied by a suitable light weight to ensure the sheets are lying flat, and resin² is poured around it, *Fig. 1*. The quickly rising viscosity of the chosen curing resin results in a penetration of approximately 1 mm locally at the outer boundaries of the sample. This penetration depth is clearly visible because of the opacity change at the edge of the sample and can, therefore, be calibrated. The open area of the porous sample, i.e. that free from resin, is evaluated so that the permeable cross-sectional area can be established. Subsequently, the sample discs are removed from the mould and placed in a dish containing the probe liquid in order to saturate the void network of the sample before placing in the permeation apparatus. The choice of liquid depends on the application. Clearly, an interactive liquid, such as water, will change the fibre structure and this must then be evaluated at equilibrium. Furthermore, highly evaporative liquids should be avoided, given the timescale necessary to perform the experimentation.

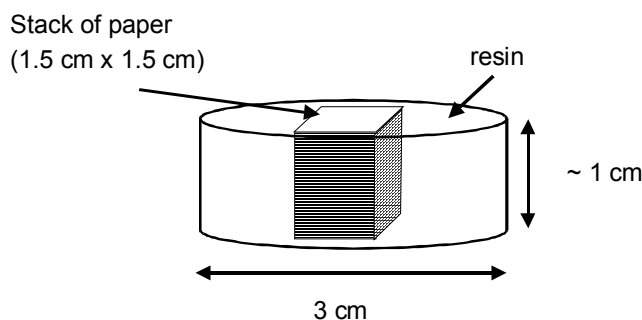


Fig. 1 Preparation of paper stack for permeability measurement.

To determine the length of the sample, l in *Eq. [1]* and *Eq. [2]*, the number of sheets embedded must be known. A correction for the gap between each sheet is then applied, based on the average caliper of the individual sheets, t' , the number of sheets, n , and the overall measured length in the embedded sample, L , to obtain a perpendicular path length through the actual permeable structure of the sheets. The apparent gaps between the sheets can be simply

¹ The PTFE-moulds used to form the cylindrical embedments were from Prüfmaschinen AG, Giessenstr. 15, CH-8953 Dietikon, Switzerland and have an inner diameter of 30 mm .

² The resin used to embed the paper samples was Technovit 4000: a product name from Heraeus Kulzer GmbH, Philipp-Reis-Strasse 8/13, D-61273 Wehrheim/Ts, Germany.

calculated as $L - nt'$, should a knowledge of the roughness interaction between sheets in the test be required. [This may be important for very micro smooth materials which are otherwise rough on the macro scale where significant volumes of air could become entrapped between the sheets during saturation by imbibition, and should be checked before and after the application of pressure during the test.]

Construction of the pressure cell

The sample under test, as prepared in the previous section, is then placed in a specially constructed pressure cell. The cell design used for the pressurised permeability experiments is shown in *Fig. 2*.

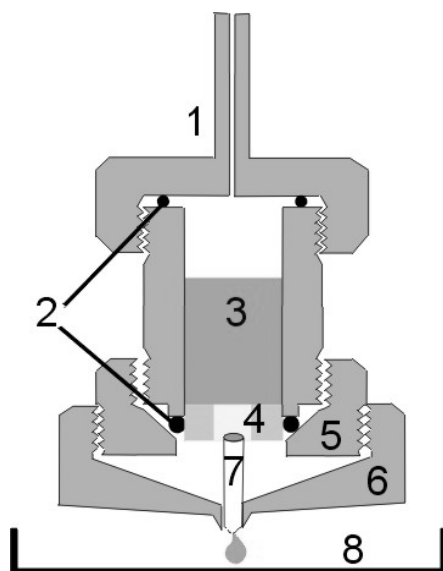


Fig. 2 Permeability measurement cell : 1) lid with pressure inlet, 2) sealing O-rings, 3) liquid cell; outer diameter = 40 mm, 4) porous sample embedded in resin disc of diameter = 30 mm, 5) fixing ring compresses the O-ring which seals the resin disc, 6) security shroud and drop collector, 7) drop captor (Teflon tubelet), 8) dish on micro-balance.

The individual parts of the cell are machined from aluminium and connect via large pitch threads to enable complete and easy assembly/disassembly. The use of the resin to embed the samples allows for rigid clamping and sealing of the sample into the pressure cell chamber. Gas over-pressure is supplied from a nitrogen bottle and passes a precision pressure reduction valve (Messer FM 62³). A Y-piece connects a digital barometer (Eurolec⁴ PR 205, 0 - 7 000 mbar) to the pressure line. The pressure cell is fixed on a tripod over a micro balance. A PC

³ Messer Griesheim GmbH, Füttingweg 34, D-47805 Krefeld, Germany, worldwide see www.messergroup.com

⁴ Eurolec Instrumentation Ltd., Cluan Enda, Dundalk, Co. Louth, Eire

samples the balance data using specially-developed software developed within Omya AG⁵. A drop captor device was needed in the base of the cell to guide the permeated liquid drops to the outlet. An important point of practical technique is that the whole chamber below the position of the sample has to be pre-wetted with the liquid so that each drop leaving the sample causes a drop to fall into the sampling dish. Once these precautions are taken the continuity of flow is ensured. Hexadecane was used in the experiments with density, $\rho = 773 \text{ kgm}^{-3}$ and viscosity, $\eta = 0.0034 \text{ kgm}^{-1}\text{s}^{-1}$. Hexadecane is non-interactive with the fibres of the paper samples.

RESULTS AND DISCUSSION

The permeability of three example papers, an LWC base paper, a standard woodfree copy paper and a multi-coated woodfree paper, was studied over a range of applied pressures. The paper properties and the permeation results are collected in Table 1. The equivalent permeation radius, r_{perm} (Eq. [1]) and the permeability constant, k (Eq. [2]), are thus determined as follows.

Flow rate at a given pressure

The permeability measurement was performed over a long enough time such that a straight line with a well-defined gradient, in respect to mass flow as a function of time, $dm(t)/dt$, at a given applied pressure across the sample, δP , was obtained. A typical result is shown in Fig. 3. Applying linear regression analysis, the constant mass flow rate was determined. It is necessary to ensure that the flow is in the necessary steady state at each constant pressure - it was seen that particular care is needed with coated samples in respect to this latter condition. The time needed can range from a few minutes for a highly permeable sample to many hours for a sample with a low permeability.

⁵ Software can be obtained on request from Dr. D. Spielmann, Omya AG Postfach 32, CH 4665 Oftringen, Switzerland

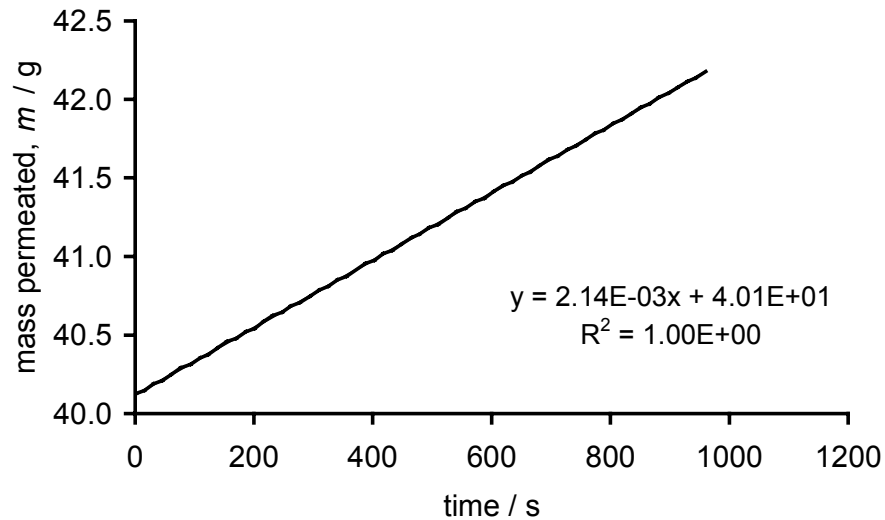


Fig. 3 Typical permeation curve, LWC base paper, $\Delta P = 3$ bar. [The excellent constancy of mass flow rate that can be achieved by the methodology is shown in this plot of actual collected data.]

Flow rate as a function of pressure

The flow rate is then determined as a function of applied pressure. At this stage it is particularly important to check for any hysteresis in the flow rate-pressure results, as previously, using a similar method to determine the permeability of porous consolidated calcium carbonate pigment tablets (Schoelkopf 2002), it was reported that there is the possibility of air being trapped within the sample. The presence of air leads to a reduced flow rate at low pressure and so a hysteresis is observed between the ramp-up and the ramp-down in pressure. Expulsion of the air, or confinement to areas that are not taking part in fluid flow, is achieved by initially applying a maximum pressure and then reducing the pressure progressively for the actual measurement series. Further ramping-up of pressure is then used to show that any hysteresis is removed. It was to be expected, therefore, that coated papers, especially with heavy coat weight, might show the same tendency toward hysteresis by entrapped air.

The ramp-up and ramp-down curve for the uncoated LWC basepaper is shown below in *Fig. 4*. Here it is confirmed that there is no problem with the air trapping phenomenon. Such is the case generally for relatively highly porous permeable samples.

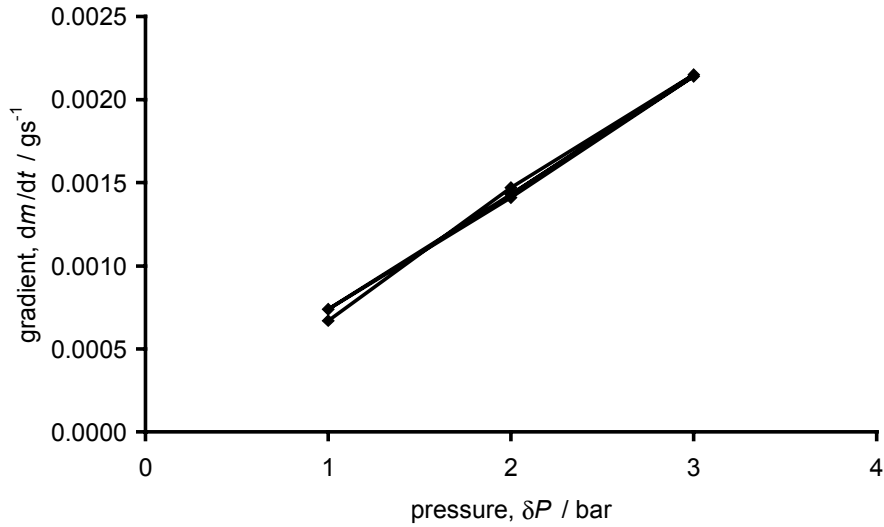


Fig. 4 Pressure hysteresis test for uncoated LWC base paper: the reproducibility of the ramp-up and ramp-down curves shows the absence of entrapped air and that the sample is in equilibrium.

The ramp-up and ramp-down of pressure is not necessary for the actual measurement of the sample. Once the possibility of hysteresis has been initially checked and eliminated if present, a suitable pressure can be established and used for a single run.

The data of mass flow rate as a function of applied pressure for the various papers are shown in Fig. 5.

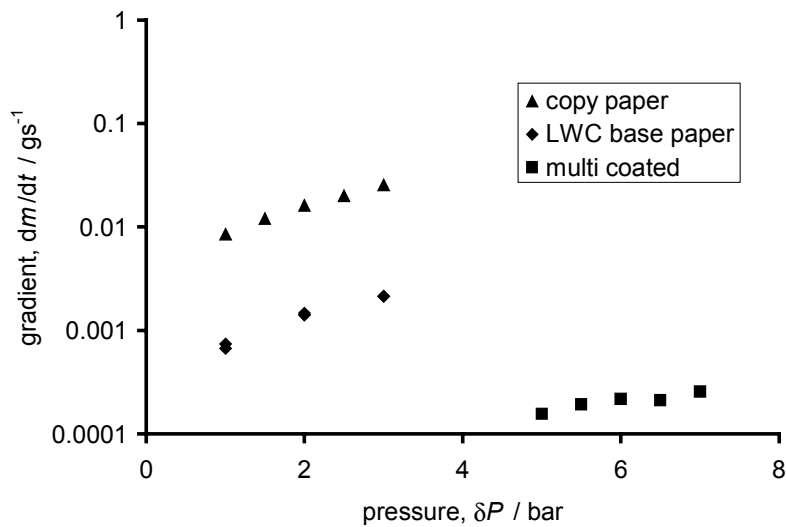


Fig. 5 Permeation mass flow rate gradients of paper samples as a function of applied pressure.

Equivalent permeability radius and Darcy permeability

Knowing the sample dimensions (length, l , and cross-sectional area, A) and the liquid properties of viscosity and density, the equivalent permeation radius per cross-sectional area can be calculated using Eq. [1] above, where $d(V(t)/A)/dt = d(m(t)/(\rho A))/dt$. These results are shown in Fig. 6.

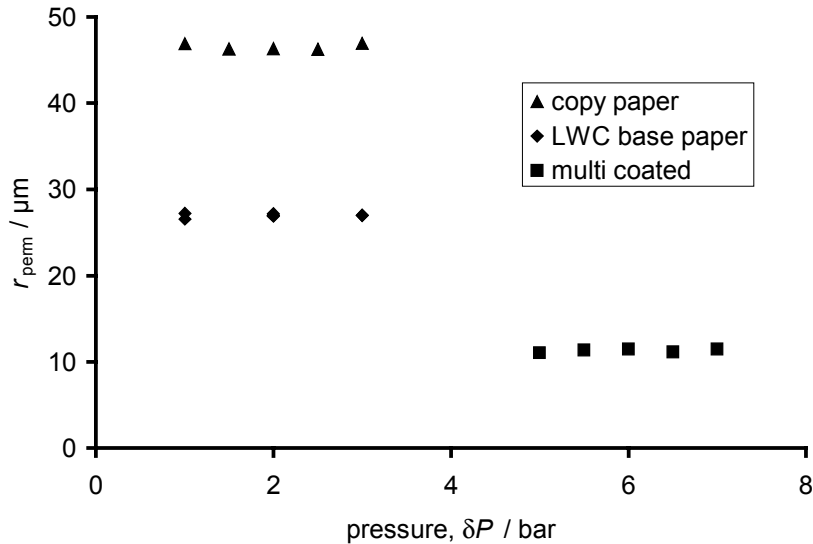


Fig. 6 Equivalent permeation radii, r_{perm} , expressed as the radius of an equivalent straight pipe that would allow the same flux of liquid according to the Poiseuille equation as seen from a square metre of the sample of length l metres under test at a differential pressure of δP bar.

The permeability, k , of these samples can be calculated using the Darcy equation, Eq. [2]. The permeabilities for the three paper samples are listed in Table 1. We include also a comparison with the Bendtsen air permeability values⁶ expressed also as the Darcy constant, k , knowing the cross section and pressure difference of the instrument using a viscosity value for air of 17.2 μPas .

⁶ Bendtsen-Messgerät SE 114 (Lorentzen & Wettre, Stockholm, Sweden)

Table 1 Summary of paper sample properties and observed permeabilities.

Sample	Basis weight /gm ⁻²	Thickness, <i>t'</i> /μm	*Darcy permeability, <i>k</i> /m ²	Bendtsen air permeability, <i>k</i> /m ²
Uncoated woodfree copy paper	80	113	1.84e-14 ± 5.51e-16	1.84e-14
LWC base paper	36	55	2.08e-15 ± 6.22e-17	1.88e-15
Multi-coated woodfree gloss	150	115	6.44e-17 ± 4.34e-18	7.40e-18

*average of at least 5 measurements ± standard deviation

It can be seen that the liquid permeabilities are in relatively close agreement with the Bendtsen air permeabilities for the uncoated papers, but the value for the multi-coated woodfree gloss paper is an order of magnitude smaller in the case of the Bendtsen. This clearly shows the effect of air compression when studying coated papers of low permeability and hence the need in such cases to use an incompressible liquid to avoid an underestimate of the coated paper permeability. Contrasting the air and liquid methods could in principle be used to estimate the amount of air stored in a paper under compression which can in turn be released after the pressure region. Such phenomena are of interest in paper coating, calendering and finishing.

Comparison with mercury intrusion porosimetry

The porous structure characteristics of the three paper types were also assessed using mercury porosimetry. The data have been corrected for mercury compression and penetrometer expansion and also for the compression of the solid phase of the sample using the software Pore-Comp⁷, (Gane et al. 1996). The intrusion curves have also been corrected to an independently measured total intrusion volume (by saturation absorption of an inert liquid, in this case hexadecane) due to the inaccuracy of the measurement at low intrusion pressures (below 0.138 MPa on these plots), referred to by the authors as mercury occlusion (Ridgway, Gane 2003), and are shown in *Fig. 7*.

⁷ A software program from the Environmental and Fluid Modelling Group, University of Plymouth, Devon, PL4 8AA, UK.

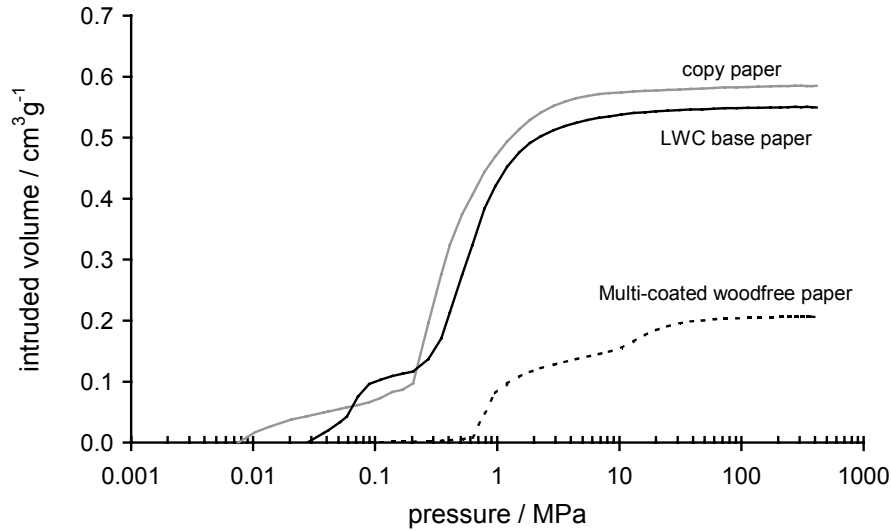


Fig. 7 Corrected mercury intrusion curves for the three papers.

These three intrusion curves show that the copy paper and the LWC uncoated base paper have the highest intrusion volumes and the largest Young-Laplace capillary diameters at the point of inflection, i.e. the largest 50 % intrusion pore size, d_{50} . In contrast, the multi-coated woodfree paper has the lowest intrusion volume and the smallest average intrusion capillary diameter. These data indicate that the copy paper and the LWC base paper are somewhat similar to each other qualitatively in respect to intrusion pore characteristics, but that the multi-coated woodfree paper has a much finer pore structure as might be expected from the fact that it is coated with a fine pigment coating structure. However, the permeability measurement shows that the equivalent permeation radius, r_{perm} , in Fig. 6, for the copy paper is significantly different from the uncoated LWC base paper. This difference is even further magnified when one considers the Darcy permeability factor (Table 1). There is, therefore, no direct correlation between permeability, porosity and Young-Laplace equivalent intrusion pore diameter. This finding illustrates the need to consider parameters of connectivity and pore shape - all of which demand the description of a porous medium in terms of a network structure in order to describe the relevance of pore structure to the observed permeability of liquids. Examples of computer modelling to capture the pore level characteristics of compacts of fine coating pigments during liquid imbibition include the use of delineated interconnected 3-D pore-throat arrays (Schoelkopf et al. 2000; Ridgway et al. 2001; Ridgway, Gane 2002). Application of these methods to permeability will form the basis of future publication.

CONCLUSIONS

A new permeation test procedure has been developed to measure the liquid permeability of fibrous and/or semi-friable porous media. Its application to sheet-like materials has been demonstrated using various grades of coated and uncoated paper. The technique removes the artefacts of random pinholes and relates directly to liquid permeation rather than the more commonly used air/gas permeation. The measurements from three papers have been presented, and the equivalent permeation radii and Darcy permeabilities have been calculated.

Permeability, as measured here using incompressible liquid, was compared with that using the Bendtsen air permeability method. It was shown that coated papers of low permeability demand the use of an incompressible liquid to avoid the compressional effect of air distorting the pressure gradient and delivering a too small permeability value.

Liquid permeability was also compared with mercury porosimetry data for the same samples, and each method was shown to indicate different properties of the porous structures, i.e. porosity and equivalent intrusion diameter alone, assuming the traditional bundle of capillaries, are not necessarily representative of the saturated permeability characteristics of a porous medium. This confirms that it is necessary to consider network structures including connectivity and pore shape and size distributions in order to correlate porosimetry with permeation properties of differing samples.

LITERATURE

Borgerding, M.F., Bodnar, J.A., and Wingate, D.E. (2000), The 1999 Massachusetts Benchmark Study Final Report.

Gane, P.A.C., Kettle, J.P., Matthews, G.P., Ridgway, C.J. (1996): Void Space Structure of Compressible Polymer Spheres and Consolidated Calcium Carbonate Paper-Coating Formulations, *Industrial and Engineering Chemistry Research*, 35 (5), 1753.

Gurley Paper Testing Instruments (2001a): Teledyne Gurley.

Heinemann, S. (1996): Bestimmung der Oberflächenrauigkeit und der Luftdurchlässigkeit von Papier nach der Bendtsen-Methode, *Das Papier* (5), 233.

ISO (1994): Paper and Board - Determination of Air Permeance (Medium Range) Part 5. Gurley Method, International Standards Organisation, 1.

L&W Bendtsen Messgerät Bedienungsanleitung (2001b): AB Lorentzen & Wettre, Kista, Sweden.

Lohmander, S., Martinez, M., Lason, L., and Rigdahl, M. (1999): Dewatering of Coating Dispersions - Model Experiments and Analysis, Advanced Coating Fundamentals Symposium, Toronto, 43.

Ridgway, C.J., Gane, P.A.C. (2002): Dynamic Absorption into Simulated Porous Structures, Colloids and Surfaces A: Physicochemical and Engineering Aspects, 206 (1-3), 217.

Ridgway, C.J., Gane, P.A.C. (2003): Bulk Density Measurement and Coating Porosity Calculation for Coated Paper Samples, Nordic Pulp and Paper Research Journal, 18(1), 24.

Ridgway, C.J., Schoelkopf, J., Matthews, G.P., Gane, P.A.C., James, P.W. (2001): The Effects of Void Geometry and Contact Angle on the Absorption of Liquids into Porous Calcium Carbonate Structures, Journal of Colloid and Interface Science, 239 (2), 417.

Rousu, S.M., Gane, P.A.C., and Eklund, D.E. (2001): Influence of Coating Pigment Chemistry and Morphology on the Chromatographic Separation of Offset Ink Constituents, Twelfth Fundamental Research Symposium, Oxford, 1115.

Schoelkopf, J. (2002), Observation and Modelling of Fluid Transport into Porous Paper Coating Structures, PhD thesis, University of Plymouth, U.K..

Schoelkopf, J., Ridgway, C.J., Gane, P.A.C., Matthews, G.P., Spielmann, D.C. (2000): Measurement and Network Modelling of Liquid Permeation into Compacted Mineral Blocks, Journal of Colloid and Interface Science, 227 (1), 119.

Torsaeter, O. and Abrahi, M. (2000): "Experimental Reservoir Engineering Laboratory Workbook", Department of Petroleum Engineering and Applied Geophysics, Norwegian University of Science and Technology.

van Brakel, J. (1975): Pore Space Models for Transport Phenomena in Porous Media Review and Evaluation with Special Emphasis on Capillary Liquid Transport, Powder Technology, 11, 205.

Vomhoff, H., Martinez, M., Norman, B. (2000): The Transversal Steady-State Permeability of a Fibre Web Compressed Between Rough Permeable Surfaces, Journal of Pulp and Paper Science, 26 (12), 428.